Supplementary Information

A. Decision-making network of spiking neurons

The network architecture

The network model in Wang (2002) (see also (Brunel and Wang 2001)) consisted of three populations of pyramidal neurons (combined total $N_E = 1600$) and one population of interneurons ($N_I = 400$). Two of the excitatory populations (each with fN_E cells, $f = 0.15$) were each sensitive to a leftward or rightward motion of the stimulus. The interneurons and the remaining $(1 - 2f)N_E$ pyramidal cells were non-selective to any of the motion stimuli. The inhibitory population acted not only to globally inhibit the excitatory cells, but also to inhibit itself.

In addition to receiving inputs from all other cells (fully-connected network), each neuron also received Poisson distributed noisy excitatory inputs from neurons outside the local cortical module. Besides mimicking *in vivo* conditions, the external input provided a main source of noise to the local network. Moreover, the overall excitatory external input, together with feedback inhibition that dominates the recurrent circuit, results in a low spontaneous firing rate for the pyramidal cells (Amit and Brunel 1997).

Neurons

Single cells were represented by a leaky integrate-and-fire (LIF) model. For each unit, the resting potential V_L, firing threshold V_{th}, and reset potential V_{reset} were set respectively to -70mV, -50mV and -55mV. The membrane leak conductance and membrane time constant for pyramidal cells were $g_L = 25$nS and $\tau_m = 20$ms, and 20nS and 10ms for interneurons. Below V_{th}, the membrane potential of the cell $V(t)$ was governed by

$$C_m \frac{dV(t)}{dt} = -g_L(V(t) - V_L) - I_{syn}(t) \ .$$

When $V(t)$ reached V_{th} the cell generated an action potential in the form of a spike (a delta function). After that, the cell stayed in a short absolute refractory period, where the membrane potential was clamped at V_{reset}, which was 2ms for pyramidal cells and 1ms for interneurons.

Synapses

The total synaptic input current to a cell, I_{syn}, came from both external (ext) inputs and recurrent (rec) synaptic connections. The recurrent inputs included both excitatory and inhibitory currents. The excitatory inputs consisted of AMPA and NMDA receptor-mediated synapses, while the inhibitory input was $GABA_A$ receptor-mediated. Thus

$$\begin{aligned}
I_{syn}(t) &= I_{ext,AMPA}(t) + I_{rec,AMPA}(t) + I_{rec,NMDA}(t) + I_{rec,GABA}(t) \\
I_{ext,AMPA}(t) &= g_{ext,AMPA}(V(t) - V_E) S_{j,ext,AMPA}(t) \\
I_{rec,AMPA}(t) &= g_{rec,AMPA}(V(t) - V_E) \sum_{j=1}^{N_E} w_j S_{j,rec,AMPA}(t) \\
I_{rec,NMDA}(t) &= \frac{g_{rec,NMDA}(V(t) - V_E)}{(1 + [Mg^{2+}] exp(-0.062V(t))/3.57)} \sum_{j=1}^{N_E} w_j S_{j,NMDA}(t) \\
I_{rec,GABA}(t) &= g_{GABA}(V(t) - V_I) \sum_{j=1}^{N_I} S_{j,GABA}(t)
\end{aligned}$$

where g was the peak synaptic conductance, S the synaptic gating variable (fraction of open channels), $V_E = 0$ the reversal potential of excitatory connectivity, and $V_I = -70$mV the reversal potential for inhibitory synapses. w was a dimensionless potentiation factor due to structured excitatory synapses (to be explained later). The sum over j was a sum over presynaptic neurons. The NMDA current was voltage-dependent and was controlled by extracellular magnesium concentration $[Mg^{2+}]$ (Jahr and Stevens 1990), which was set at 1mM. The peak conductances for excitatory synapses to pyramidal cells, in units of μS, are here chosen to be $g_{rec,AMPA} = 0.0005$, $g_{ext,AMPA} = 0.0021$, $g_{NMDA} = 0.000165$, and $g_{rec,AMPA} = 0.00004$, $g_{ext,AMPA} = 0.00162$, $g_{NMDA} = 0.00013$ to the interneurons. The peak conductances for inhibitory synapses to pyramidal cells and interneurons, g_{GABA}, are 0.0013μS and 0.001μS respectively. These peak conductance values are comparable to experimental measurements (e.g. (Destexhe et al. 1998)). The dynamics for the synaptic gating variables are

$$
\begin{aligned}
\frac{dS_{j,AMPA}(t)}{dt} &= -\frac{S_{j,AMPA}(t)}{\tau_{AMPA}} + \sum_k \delta(t - t_j^k) \\
\frac{dS_{j,GABA}(t)}{dt} &= -\frac{S_{j,GABA}(t)}{\tau_{GABA}} + \sum_k \delta(t - t_j^k) \\
\frac{dS_{j,NMDA}(t)}{dt} &= -\frac{S_{j,NMDA}(t)}{\tau_{NMDA,decay}} + \alpha x_j(t)(1 - S_{j,NMDA}(t)) \\
\frac{dx_j(t)}{dt} &= -\frac{x_j(t)}{\tau_{NMDA,rise}} + \sum_k \delta(t - t_j^k)
\end{aligned}
$$

The summation of delta functions denoted the sum of spikes generated from presynaptic neurons. The time constants were $\tau_{AMPA} = 2$ms, $\tau_{NMDA,decay} = 100$ms, $\tau_{NMDA,rise} = 2$ms (Hestrin et al. 1990; Spruston et al. 1995), $\tau_{GABA} = 5$ms, (Salin and Prince 1996; Xiang et al. 1998), and $\alpha = 0.5\text{ms}^{-1}$. The rise time for AMPA and GABA (< 1ms) were assumed to be instantaneous. Spikes from external of the network were assumed to go through AMPA receptors. For simplicity, we did not incorporate synaptic latency (0.5ms used in Wang (2002)).

Structure of recurrent excitatory synapses between pyramidal cells

Excitatory synapses within a selective population were chosen to be relatively stronger than excitatory synapses to cells outside the selective population. This particular structure was similar to the "Hebbian" rule where cells that tend to fire together form stronger synapses. These relatively strong synapses came in the form of a potentiation factor $w = w_+ > 1$. To ensure that all excitatory neurons maintain the same spontaneous mean firing rate, compensation from the unpotentiated synapses were needed. This was done by introducing a "depression" factor $w = w_- = 1 - f(w_+ - 1)/(1 - f) < 1$ for the synapses between two different selective populations, and for synapses between the nonselective population to selective ones (Amit and Brunel 1997). For all other connections, $w = 1$. Unless specified otherwise, we used $w_+ = 1.7$ (Wang 2002).

B. Single-cell input-output relation

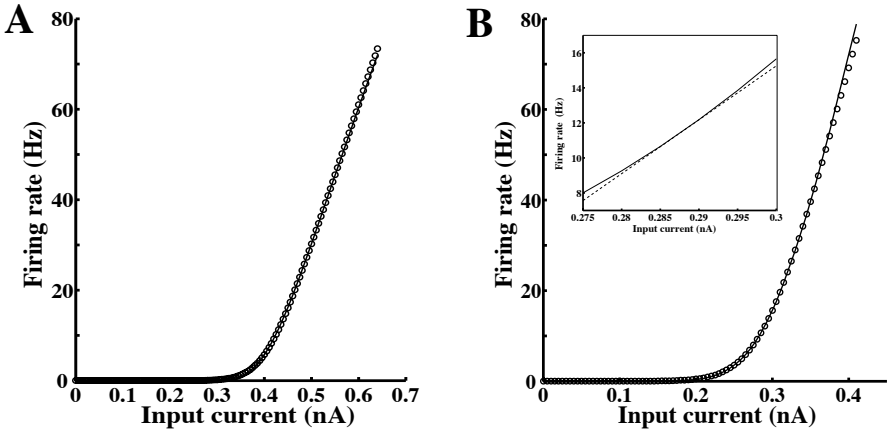

Supplemental Figure 1. Input-output relation of a pyramidal cell (A), and an interneuron (B). Bold lines are plotted using the first-passage time formula of a LIF model (Eq. 1). Circles are fits using Eq. 2. Inset: close-up of the input-output relation for an interneuron. Dashed line: linear approximation using Eq. 9.

C. Average gating variable of NMDA receptors vs presynaptic firing rate

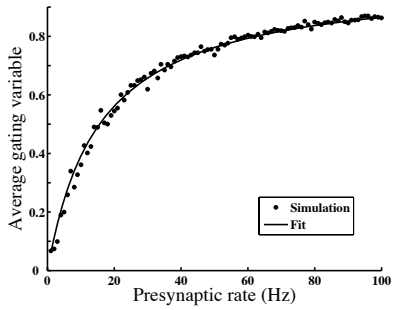

Supplemental Figure 2. Average fraction of open channels of NMDA receptor vs average presynaptic firing rate. The input, through the NMDA receptor mediated conductance, consists of delta-like spikes with the interspike interval described by a Poisson distribution. Bold curve: fit using Eq. 8.

D. Effective transfer functions

The single-cell input-output relation, $r_i = \phi(I_i)$ (Eq. 2), where $i = 1, 2$, is nonlinear and is a function of $I_i(S_1, S_2, r_1, r_2)$ (Eqs. 14 and 15). It is non-trivial to solve r_1 and r_2 as functions of only S_1 and S_2. A typical way to approach this problem is to solve, at every time step self-consistently. This is done by iteratively solving r_1 and r_2 with known values of S_1 and S_2. However, the computation done this way is costly. Here, we shall follow a different, less elegant but computationally faster approach. We want to solve for ϕ as a function of each of its variable separately, and obtain a simplified (but effectively similar) form which we label here as H.

Now we define two new variables

$$\begin{aligned} x_1 &= J_{N,11}S_1 - J_{N,12}S_2 + I_0 + I_1 \\ x_2 &= J_{N,22}S_2 - J_{N,21}S_1 + I_0 + I_2 \ . \end{aligned}$$

For any pair of x_1, x_2, we can numerically solve for r_1, r_2 and thus fit each of the latter with an equivalent response function in terms of the two new variables:

$$\begin{aligned} r_1 &= H_1(x_1, x_2) \\ r_2 &= H_2(x_2, x_1) \ . \end{aligned}$$

By doing this, we avoid running into self-consistency calculations at every time step. With the external input now implicitly contained in x_1 and x_2, H_1 and H_2 should have the same form even when the inputs (e.g. stimulus strength or coherence level) are varied. This fitting holds true even when $J_{N,11}$, $J_{N,12}$, w_+, and c' are changed. We have neglected the fact that the functions H_1 and H_2 can also depend on the couplings $J_{A,11} = J_{A,22}$ and $J_{A,12} = J_{A,21}$ through AMPA synapses. For example, $J_{A,11}$ generally increases the gain of H_1 (supplemental Fig. 3A) while $J_{A,12}$, as with x_2, shifts H_1 laterally (supplemental Fig. 3B).

Thus, if H_1 (H_2) can be fitted by a function of $J_{A,11}$ ($J_{A,22}$) and $J_{A,12}$ ($J_{A,21}$), no matter how the network parameters (e.g. w_+, synaptic conductances) are varied, the above equations will still hold true. These functions are fitted with a similar form to their corresponding original input-output relations (Eq. 2), but with the coefficients now as functions of $J_{A,11}$ and

$J_{A,12}$:

$$\begin{aligned} r_1 &= H_{J_{A,11},J_{A,12}}(x_1, x_2) \\ &= \frac{a(J_{A,11})x_1 - f_A(J_{A,12}, x_2) - b(J_{A,11})}{1 - exp[-d(J_{A,11})(a(J_{A,11})x_1 - f_A(J_{A,12}, x_2) - b(J_{A,11}))]} \\ r_2 &= H_{J_{A,22},J_{A,21}}(x_2, x_1) \\ &= \frac{a(J_{A,22})x_2 - f_A(J_{A,21}, x_1) - b(J_{A,22})}{1 - exp[-d(J_{A,22})(a(J_{A,22})x_2 - f_A(J_{A,21}, x_1) - b(J_{A,22}))]} \end{aligned}$$

where a, b, d are new parameters chosen to fit the numerical solutions. Because of inhibitory effects from J and x, the function f_A, shifts the function H laterally. For simplicity, we shall approximate the parameters a, b and d to be linearly dependent on $J_{A,11}$ or $J_{A,22}$. For population 1,

$$\begin{aligned} a(J_{A,11}) &= 239400J_{A,11} + 270 \ ((\text{VnC})^{-1}) \\ b(J_{A,11}) &= 97000J_{A,11} + 108 \ (\text{Hz}) \\ d(J_{A,11}) &= -30J_{A,11} + 0.1540 \ (\text{s}) \ , \end{aligned}$$

The "shift" function f_A due to AMPA can be approximated by a threshold-linear function as follows:

$$f_A(J_{A,12}, x_2) = J_{A,12}(-276x_2 + 106)\theta(x_2 - 0.4) \text{ Hz}$$

where $\theta(x)$ is 0 if $x < 0$ and 1 if $x \geq 0$. By symmetry, the same functional forms apply to population 2.

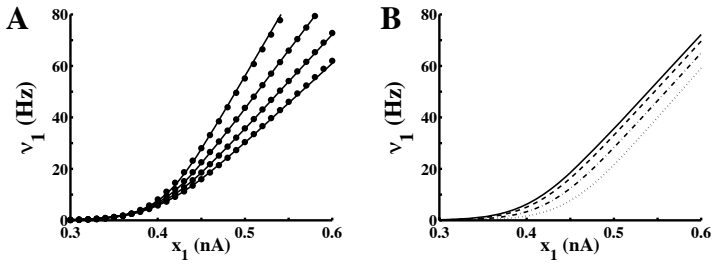

Supplemental Figure 3. Numerical fits for effective input-output relation of cells in competiting population. (A). As $J_{A,11} = J_{A,22}$ increases the gain increases. Bold lines: numerical solutions for $J_{A,11} = J_{A,22} = 0, 0.0005$, 0.0010, 0.0015, 0.002nAHz^{-1}. The larger $J_{A,11} = J_{A,22}$ is, the higher the gain. Circles: fits. (B). An increase of x_2 or $J_{A,12} = J_{A,21}$ shift the r_1-vs-x_1 curve laterally rightward. From left to right: $J_{A,12} = J_{A,21} = 0$, 0.00005, 0.00010, 0.00015nAHz^{-1}.

E. Condition for diffusion-like process of decision-making

To simplify the calculations, we assume that (i) the recurrent synapses have only NMDAR-mediated conductances; (ii) the inhibition and firing rates are instantaneous as in our two-variable reduced model. Then the dynamical equations for the system become:

$$\begin{aligned}\frac{dS_1}{dt} &= G_1(S_1, S_2) = -\frac{S_1}{\tau_S} + (1 - S_1)\gamma\nu_1 \\ \frac{dS_2}{dt} &= G_2(S_2, S_1) = -\frac{S_2}{\tau_S} + (1 - S_2)\gamma\nu_2\end{aligned}$$

where

$$\begin{aligned}\nu_1 &= \phi_1(I_{syn,1} = J_{11}S_1 - J_{12}S_2 + I_0 + I_1) \\ \nu_2 &= \phi_2(I_{syn,2} = J_{22}S_2 - J_{21}S_1 + I_0 + I_2)\end{aligned}$$

where J_{ij} is the usual recurrent synaptic couplings with $J_{11} = J_{22}$, $J_{12} = J_{21}$.

Assuming that $(\hat{S}_1, \hat{S}_2)$ is the saddle steady-state, then a small perturbation from this unstable steady-state to $(\hat{S}_1 + \epsilon_1, \hat{S}_2 + \epsilon_2)$, gives

$$\begin{aligned}\frac{d\epsilon_1}{dt} &= G_1(\hat{S}_1, \hat{S}_2) + \frac{\partial G_1}{\partial S_1}\Big|_{(\hat{S}_1,\hat{S}_2)} d\epsilon_1 + \frac{\partial G_1}{\partial S_2}\Big|_{(\hat{S}_1,\hat{S}_2)} d\epsilon_2 \\ &= -\frac{\epsilon_1}{\tau_S} + \gamma\epsilon_1\left(-\hat{\nu_1} + (1 - \hat{S}_1)J_{11}\partial\hat{\phi}_1\right) - (1 - \hat{S}_1)J_{12}\gamma\epsilon_2\partial\hat{\phi}_1\end{aligned}$$

and similarly,

$$\frac{d\epsilon_2}{dt} = -\frac{\epsilon_2}{\tau_S} + \gamma\epsilon_2\left(-\hat{\nu_2} + (1 - \hat{S}_2)J_{11}\partial\hat{\phi}_2\right) - (1 - \hat{S}_2)J_{12}\gamma\epsilon_1\partial\hat{\phi}_2$$

where $\hat{\nu}$'s, $\hat{S}$'s and the partial derivatives are evaluated at the steady-state. $\partial\hat{\phi}_i$ is the abbreviation of $\partial\phi_i/\partial I_{syn,i}$ at the steady-state.

By defining a new variable $\Delta\epsilon$, such that $\Delta\epsilon \equiv \epsilon_1 - \epsilon_2$, we can combine the above two equations:

$$\frac{d\Delta\epsilon}{dt} = -\frac{\Delta\epsilon}{\tau_S} + (\omega_{11} + \omega_{12})\Delta\epsilon$$

where we have assumed $I_1 = I_2$, and thus $\hat{\nu_1} = \hat{\nu_2} \equiv \hat{\nu}$, $\hat{S_1} = \hat{S_2} \equiv \hat{S}$, $\partial\hat{\phi_1} = \partial\hat{\phi_2} \equiv \partial\hat{\phi}$, $\omega_{11} \equiv \left(-\hat{\nu} + (1-\hat{S})J_{11}\right)\gamma\partial\hat{\phi}$ and $\omega_{22} \equiv (1-\hat{S})J_{12}\gamma\partial\hat{\phi}$.

The decision-making process can become a one-dimensional diffusion process provided the following condition is satisfied:

$$\frac{1}{\tau_S} = \omega_{11} + \omega_{12} \ .$$

If the synapses do not saturate (e.g. at low activities), then it can be shown that the above condition means a balance between the sum of recurrent couplings and the decay term.

We shall now show that this condition is equivalent to the bifurcation of the saddle steady-state (e.g. from the stable spontaneous steady-state). The Jacobian matrix of the perturbed system about the saddle steady-state is:

$$J_\epsilon = \left[\begin{array}{cc} \frac{\partial G_1}{\partial S_1} & \frac{\partial G_1}{\partial S_2} \\ \\ \frac{\partial G_2}{\partial S_1} & \frac{\partial G_2}{\partial S_2} \end{array} \right]_{(\hat{S_1},\hat{S_2})}$$

where the matrix entries, evaluated at the saddle steady-state, are found to be

$$\begin{aligned} \frac{\partial G_1}{\partial S_1}\Big|_{(\hat{S_1},\hat{S_2})} &= -\frac{1}{\tau_S} + \omega_{11} = \frac{\partial G_2}{\partial S_2}\Big|_{(\hat{S_1},\hat{S_2})} \\ \frac{\partial G_1}{\partial S_2}\Big|_{(\hat{S_1},\hat{S_2})} &= -\omega_{12} = \frac{\partial G_2}{\partial S_1}\Big|_{(\hat{S_1},\hat{S_2})} \end{aligned}$$

The two eigenvalues of this Jacobian matrix are

$$\lambda_\pm = -\frac{1}{\tau_S} + (\omega_{11} \pm \omega_{12})$$

where $\lambda_+ > 0$ and $\lambda_- < 0$ at a saddle steady-state. Close to the bifurcation point, $\lambda_+ \to 0^+$, i.e. $\frac{1}{\tau_S} \approx \omega_{11} + \omega_{12}$. Thus, we have shown that by bringing the system near the bifurcation point, the model is mathematically equivalent to having a one-dimensional diffusion process of making decisions. This argument is strengthened if we can create fast dynamics along the stable manifold since $\tau_{stable} = |\lambda_-|^{-1} = (1/\tau_S - \omega_{11} + \omega_{12})^{-1}$. This can be achieved if we have a smaller time constant for the dynamical equations (e.g. AMPA) or stronger inhibition.

F. Oscillations in the decision-making network

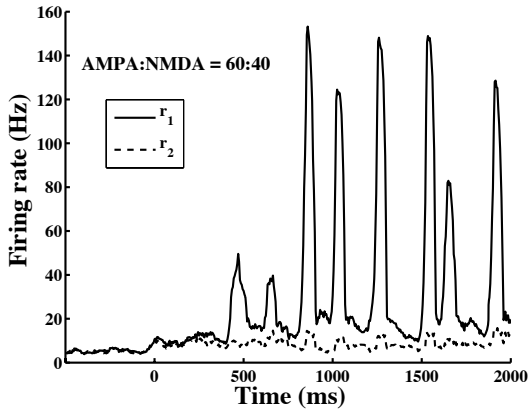

Supplemental Figure 4. Oscillations occur in the two selective populations' firing rate, r_1 and r_2, when the fraction of NMDA at the recurrent synapses is low.

References

Amit, D. J. and N. Brunel (1997). Model of global spontaneous activity and local structured activity during delay periods in the cerebral cortex. *Cereb. Cortex 7*, 237–252.

Brunel, N. and X.-J. Wang (2001). Effects of neuromodulation in a cortical network model. *J. Comput. Neurosci. 11*, 63–85.

Destexhe, A., Z. F. Mainen, and T. J. Sejnowski (1998). Kinetic models of synaptic transmission. In C. Koch and I. Segev (Eds.), *Methods of Neuronal Modeling (2nd edition)*. MIT Press (Cambridge, MA).

Hestrin, S., P. Sah, and R. A. Nicoll (1990). Mechanisms generating the time course of dual component excitatory synaptic currents recorded in hippocampal slices. *Neuron 5*, 247–253.

Jahr, C. E. and C. F. Stevens (1990). Voltage dependence of nmda-activated macroscopic conductances predicted by single-channel kinetics. *J. Neurosci. 10*, 3178–3182.

Salin, P. A. and D. A. Prince (1996). Spontaneous gaba$_A$ receptor mediated inhibitory currents in adult rat somatosensory cortex. *J. Neurophysiol. 75*, 1573–1588.

Spruston, N., P. Jonas, and B. Sakmann (1995). Dendritic glutamate receptor channel in rat hippocampal CA3 and CA1 pyramidal neurons. *J. Physiol. 482*, 325–352.

Wang, X.-J. (2002). Probabilitic decision making by slow reverberation in cortical circuits. *Neuron 36*, 955–968.

Xiang, Z., J. R. Huguenard, and D. A. Prince (1998). GABA$_A$ receptor mediated currents in interneurons and pyramidal cells of rat visual cortex. *J. Physiol. 506*, 715–730.